Journal of Zhejiang University SCIENCE A
ISSN 1009-3095 (Print); ISSN 1862-1775 (Online)
www.zju.edu.cn/jzus; www.springerlink.com
E-mail: jzus@zju.edu.cn

# Metal hydride work pair development and its application on automobile air conditioning systems*

QIN Feng†1, CHEN Jiang-ping[1], ZHANG Wen-feng[2], CHEN Zhi-jiu[1]

([1]*Institute of Refrigeration and Cryogenic Engineering, Shanghai Jiao Tong University, Shanghai 200030, China*)

([2]*Research Center, Zhejiang Yinlun Machinery Co., Ltd., Tiantai 317200, China*)

†E-mail: fqin@mail.sjtu.edu.cn

Received May 20, 2006; revision accepted Aug. 21, 2006

**Abstract:** Aiming at developing exhaust gas driving automobile air conditioning systems, a hydride pair $LaNi_{4.61}Mn_{0.26}Al_{0.13}$/$La_{0.6}Y_{0.4}Ni_{4.8}Mn_{0.2}$ was developed working at 393~473 K/293~323 K/263~273 K. Property tests showed that both alloys have flat plateau slopes and small hystereses; system theoretical coefficient of performance (COP) is 0.711. Based on this work pair, a function proving automobile metal hydride refrigeration system was constructed. The equivalent thermal conductivities of the activated reaction beds were merely 1.1~1.6 W/(m·K), which had not met practical requirement. Intermittent refrigeration cycles were achieved and the average cooling power was 84.6 W at 423 K/303 K/273 K with COP being 0.26. By altering cycling parameters, experiment data showed that cooling power and system COP increase with the growth of heat source temperature as well as pre-heating and regeneration time while decrease with heat sink temperature increment. This study confirms the feasibility of automobile metal hydride refrigeration systems, while heat transfer properties of reaction beds still need to be improved for better performance.

**Key words:** Metal hydride, Air conditioning, Reaction bed, Automobile, Coefficient of performance (COP)
**doi:**10.1631/jzus.2007.A0197 **Document code:** A **CLC number:** TB6; TK91

## INTRODUCTION

Metal hydrides are special alloys which absorb and desorb hydrogen reversibly. At room temperature, metal hydrides could absorb as much hydrogen as liquid hydrogen of the same volume under much lower pressure and much higher temperature (Güther and Otto, 1999). Massive reaction heat is generated accompanying this reaction, which could be used for waste heat recovery, solar energy utilization and refrigeration with no side effect to environment (Izhvanov *et al*., 1996).

Conventional automobile air conditioners mostly adopt R134a as work medium and are driven by engines, which exacerbates energy consumption and emission (Bedbak and Gopal, 2005). In order to solve these problems and make full utilization of fuels, the environmental metal hydride air conditioners driven by exhaust gas are considered to be adopted in automobiles. The key points of these air conditioners are hydride work pairs and reaction bed structures.

In this study, a $LaNi_5$ type work pair was developed and tested. Based on this hydride pair, cylindrical type reaction beds were designed, a function proving intermittent air conditioning system was developed and analyzed with heat conducting oil as heat source and water as heat sink.

## SYSTEM FUNDAMENTALS

Reversible hydride reaction could be written as (Oi *et al*., 2004),

* Project (No. 50276063) supported by the National Natural Science Foundation of China

$$M+(\alpha/2)H_2 \leftrightarrow MH_\alpha+\Delta H, \quad (1)$$

where M and MH represent elemental metal/metal alloy and metal hydride, $\Delta H$ is reaction enthalpy, $\alpha$ is hydrogen atom number. Refrigeration cycles could be attained by applying two hydrides with different hydriding properties. Fig.1 shows a cycle of heat driving metal hydride refrigeration systems. High temperature metal hydride $M_H$ and low temperature metal hydride $M_L$ with different hydrogen absorption properties are coupled to form a work pair. First $M_H$ is heated from heat sink temperature $T_M$ to drive heat source temperature $T_H$ so that its hydrogen desorption pressure exceeds that of $M_L$, thus $M_H$ desorbs hydrogen to $M_L$ and absorbs heat $Q_H$ from driving heat source; simultaneously, $M_L$ rejects reaction heat $Q_{M1}$ generated during hydrogen absorbtion to heat sinks. Then $M_H$ is cooled to $T_M$, and its hydrogen pressure drops below that of $M_L$, thus $M_L$ releases hydrogen to $M_H$ and absorbs heat $Q_L$ for cooling down surrounding temperature to refrigeration temperature $T_L$, accompanied by the delivery of reaction heat $Q_{M2}$ from $M_H$ to heat sinks. Obviously it is discontinuous due to the cold energy generated by a couple of reaction beds, consequently at least two couples of reaction beds are needed with reverse work phases for sequential refrigeration (Ahmed and Murthy, 2004).

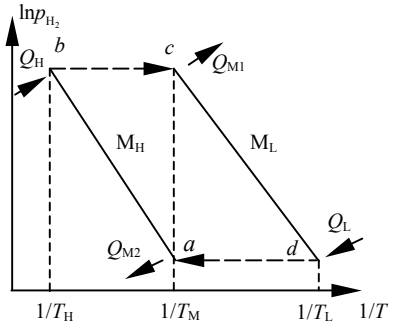


**Fig.1 Metal hydride refrigeration cycle**

## HYDRIDE PREPARATION AND CHARACTERIZATION

### Work pair preparation

Metal hydrides are the core components of metal hydride refrigeration systems. In order to ensure good system performance, metal hydrides should meet the following requirements: large effective hydrogen storage and reaction heat, fast reaction kinetics, flat reaction plateaus, small hystereses, suitable pressure gradients and affordable costs. On designing the hydride pair, we take exhaust gas driving automobile air conditioners located before exhaust mufflers as the object. Exhaust gas there is usually at a temperature of 393~573 K depending on operation conditions, thus the minimum driving temperature should not exceed 393 K; since summer environmental temperature is within 293~323 K in most parts of China, medium temperature is chosen in this range. Therefore, the work temperatures of this refrigeration system are selected as 393~473 K/293~323 K/263~273 K. Considering the above demands, $LaNi_5$ type alloys are selected as matrix, and certain metal additives are adopted for improvement. For high temperature alloy $M_H$, Al and Mn are added to reduce equilibrium pressures and depress hystereses (Nakamura *et al.*, 1997); for low temperature alloy $M_L$, Y is added to increase equilibrium pressures while Mn is added to improve reaction kinetics (Nakamura *et al.*, 1996). From repeated trials, $LaNi_{4.61}Mn_{0.26}Al_{0.13}$/$La_{0.6}Y_{0.4}Ni_{4.8}Mn_{0.2}$ were developed respectively as the high/low temperature hydrides. High frequency induction melting was adopted for their preparation, then both were treated by 1323 K annealing for 10 h then quenched in ice water.

### Work pair characterization

P-C isotherms and reaction kinetics of the work pair were measured with a Sieverts apparatus (Kapischke and Hapke, 1998). Fig.2 shows the tested P-C isotherms of $M_H$ and $M_L$ within work temperatures. This figure shows that the effective hydrogen contents of both two alloys are around 0.6 mol H/mol alloy, which is satisfactory for practice. Both equilibrium hydrogen pressures are much less than 4 MPa in the test range, which facilities beds sealing.

The slope factor $P_f$ and hysteresis factor $H_f$ are respectively defined as (Srivastava and Srivastava, 1999):

$$P_f=\mathrm{d}\ln p_d/\mathrm{d}(H/M), \quad (2)$$

$$H_f=\ln(p_a/p_d), \quad (3)$$

where $p_a$ and $p_d$ are hydrogen absorption and desorption equilibrium pressures, respectively; H/M is atom ratio of hydrogen to alloy. The $P_f$ and $H_f$ were

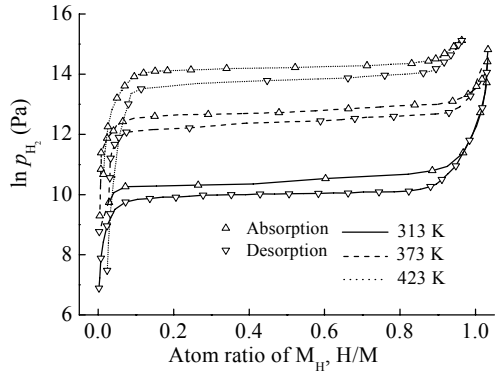


(a)

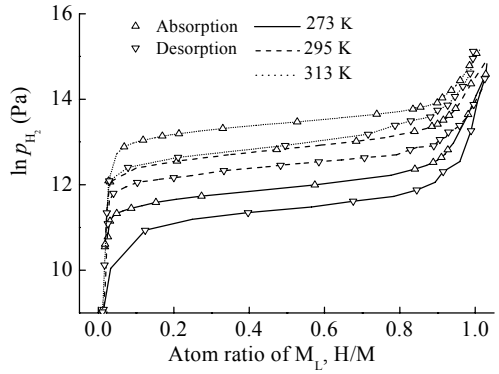


(b)

**Fig.2 P-C isotherms of $LaNi_{4.61}Mn_{0.26}Al_{0.13}$ as $M_H$ (a) and $La_{0.6}Y_{0.4}Ni_{4.8}Mn_{0.2}$ as $M_L$ (b)**

calculated in Table 1. These factors are relatively small compared with those of $LaNi_5$, which reveals that the constitution and preparation process of the hydride pair have effectively depressed segregation during crystallization.

**Table 1 Plateau slope and hysteresis factors**

| Metal hydrides | $LaNi_{4.61}Mn_{0.26}Al_{0.13}$ | | | $La_{0.6}Y_{0.4}Ni_{4.8}Mn_{0.2}$ | | |
|---|---|---|---|---|---|---|
| | 313 K | 373 K | 423 K | 273 K | 295 K | 313 K |
| $P_f$ | 0.360 | 0.768 | 0.708 | 1.314 | 0.960 | 1.080 |
| $H_f$ | 0.470 | 0.477 | 0.480 | 0.397 | 0.392 | 0.388 |

Based on the derived P-C isothermal data, the Van't-Hoff diagram of the work pair is drawn in Fig.3, in which the bond lines stand for the designed refrigeration cycle. According to Van't-Hoff equation (Kapischke and Hapke, 1998):

$$\ln p = -\Delta H/RT + \Delta S/R, \quad (4)$$

the reaction enthalpy during absorption $\Delta H$ is respectively calculated as −37.8 and −27.1 kJ/mol $H_2$ for the two hydrides, and absorption reaction entropy $\Delta S$ respectively is −111.7 and −102.6 J/(mol $H_2$·K).

The theoretical COP for the refrigeration system is defined as (Willers and Groll, 1999):

$$COP = \Delta H_{L,d}/\Delta H_{H,d}, \quad (5)$$

where, $\Delta H_{L,d}$ and $\Delta H_{H,d}$ are reaction enthalpy of $M_L$ and $M_H$ during desorption respectively. Substituting derived data into Eq.(5), the theoretical COP of $LaNi_{4.61}Mn_{0.26}Al_{0.13}/La_{0.6}Y_{0.4}Ni_{4.8}Mn_{0.2}$ refrigeration system is calculated as 0.711. The ideal minimum refrigeration temperature from Fig.3 reaches as low as 242 K at high temperature being 423 K and medium temperature 303 K.

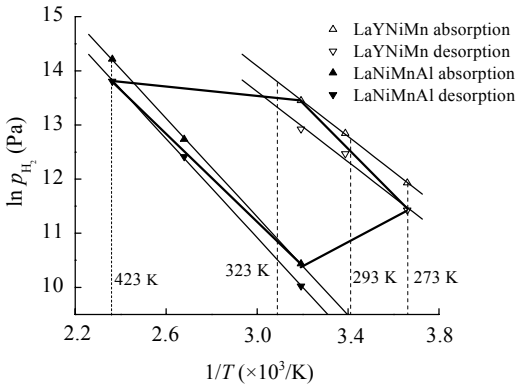


**Fig.3 Van't-Hoff diagram**

## BED DESIGN AND HEAT TRANSFER PROPERTIES

### Reaction bed design

Reaction beds are crucial for metal hydride refrigeration systems. They should be firm enough to endure hydride expansion and thermal shock, while beds weight should be as light as possible to reduce gross thermal capacity. Moreover, good heat and mass transfer properties are crucial to improve reaction kinetics. Considering above demands, a cylindrical shaped reaction bed was designed as shown in Fig.4. The bed wall was made of stainless steel 500 mm in length and ∅75 mm in outer diameter. Two pieces of flanges were adopted at cylinder edges for

sealing. A stainless steel hollow sintered filter with 2 μm nominal pore size was fixed inside the cylinder. The filter prevents hydride powder inside from floating out, and the donut chamber between the wall and the filter ensures extensive contact areas at whole length. A finned copper tube was inserted through the filter, dividing the reaction areas into several sections. In order to measure hydride temperatures, four pieces of single-point and two pieces of double-point K type armored thermocouples were inserted axially through flanges 200 mm inside the bed. The single-point thermocouples were symmetrically installed in one flange with different diameters to measure radial temperature distributions, and double-point thermocouples were installed in two flanges to measure axial temperature distributions.

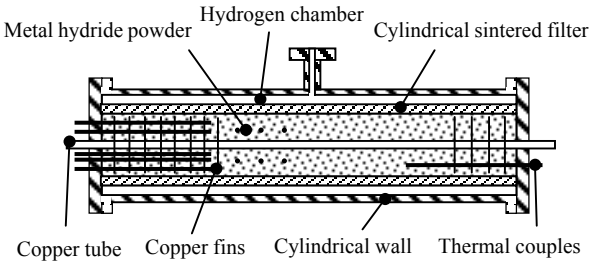


**Fig.4 Reaction bed structure**

Metal hydrides were ground and filtered by 10 mesh screen. Each high and low temperature bed was filled with 2.75 kg $LaNi_{4.61}Mn_{0.26}Al_{0.13}$ or $La_{0.6}Y_{0.4}Ni_{4.8}Mn_{0.2}$ respectively, with volume packing density around 42%. The filled hydrides were activated through three absorption/desorption cycles with 4.0 MPa high purity hydrogen at room temperature, each cycle lasting for 6 h.

**Heat transfer property experiments**

Heat transfer coefficients of the reaction beds are an important factor to affect cooling power. According to reading the temperatures acquired by thermal couples inside beds, the approximate radial equivalent thermal conductivities could be calculated based on one-dimensional Fourier stationary heat transfer equation. A $LaNi_{4.61}Mn_{0.26}Al_{0.13}$ reaction bed was experimented. In order to increase radial heat transfer quantity, the sintered filter was disassembled, the space between finned tube and outer wall was packed with alloy keeping volume packing density of 42%. The reaction bed was put in a water tank to stabilize the outer wall temperature. High temperature heat conducting oil was adopted for heat source. The test was undergone first for inactivated alloy, then the bed was activated and measured with different hydrogen contents. The results are shown in Table 2 with the maximum relative error of 10.3%.

**Table 2 Thermal conductivities of the reaction bed**

| Hydride state | Thermal conductivity [W/(m·K)] |
|---|---|
| Vacuum, inactivated | 0.61 |
| LaNiMnAl-1.25H | 1.12 |
| LaNiMnAl-2.5H | 1.35 |
| LaNiMnAl-5.0H | 1.56 |

The experiment showed that the reaction bed has better heat transfer properties than pulverized hydride of about 0.1 W/(m·K) (Kim *et al*., 2001), which is attribute to the finned tube. However, this thermal conductivity can not satisfy practical usage as 5~8 W/(m·K) (Sánchez *et al*., 2003), which implies that the extension of heat transfer interfaces is still too limited by fins with 20 mm intervals. Whereas, if we only increase fins per unit length, the bed heat capacity would be extensively increased, resulting in the obvious depression of cold output. Thus bed thermal conductivities should be further improved by optimizing bed structures or upgrading alloy thermal conductivity itself by special treatment.

## REFRIGERATION SYSTEMS DESIGN AND PERFORMANCE TEST

**Refrigeration system design**

Originally, a continuous refrigeration system was planned to be built with two couples of reaction beds working with reverse phases, so two pairs of high temperature and low temperature beds were prepared. However, equivalent thermal conductivity test showed that the heat transfer properties of the reaction beds were not practically satisfactory, leading to a low hydriding process and indistinct temperature drop for cooled water (Oi *et al*., 2004). Therefore, the two high and low temperature beds were assembled respectively in series to build an intermittent refrigeration system. The revised scheme

is shown in Fig.5. The whole system was composed of four reaction beds, a hydrogen loop, a heat conducting oil loop, a water loop and sensors/data acquisition instruments. High temperature and low temperature reaction beds were connected by hydrogen pipes. Valves were installed to control hydrogen flow directions. Four 0~4 MPa Druck PTX1400 pressure transmitters were fixed to record pressure variations. Hydrogen charge and vacuumization branches were also added. Heat was supplied to high temperature reaction beds by heat conducting oil drawn from the high temperature oil bath, and cold in low temperature reaction beds was absorbed by cooled water bath. Reaction heat of both reaction beds was taken away by medium temperature baths. Oil and water flows were controlled by cooperating function of eight valves in the loops. An LWGY-10A turbine flow meter was adopted for flow measurement, self-calibrated 4 wire PT100 thermal resistances were used for acquisition of inlet and outlet temperatures. A Keithley 2700 data acquisition instrument was adopted for data acquisition, analysis and storage.

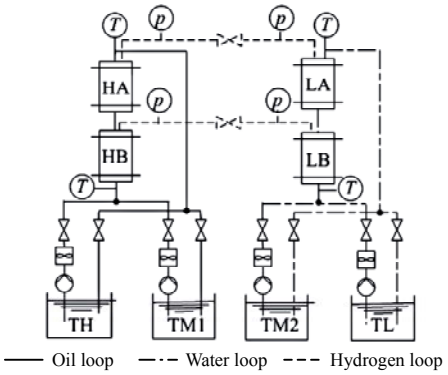


HA, HB: High temperature bed; LA, LB: Low temperature bed; TH: High temperature oil, heat source; TM1: Middle temperature oil, heat sink; TM2: Cooling water, heat sink; TL: Cooled water, heat source

**Fig.5 Metal hydride refrigeration system**

## Cycle performance test

First activated the reaction beds and then charged each high temperature reaction bed with 16 mol pure hydrogen to form $LaNi_{4.61}Mn_{0.26}Al_{0.13}$-5.0H, then began cycle performance test as follows: first opened corresponding valves to let hot oil and cooling water flow respectively through high and low temperature reaction beds for a certain time for pre-heating, the temperature of $M_H$ rose from $T_M$ to $T_H$ while $M_L$ from $T_L$ to $T_M$; then opened the hydrogen valves immediately to start regeneration period while $M_H$ absorbed $Q_H$ from hot oil and $M_L$ released $Q_{M1}$ to cooling water. After the set time intervals, closed the hydrogen valves and pumped the middle temperature oil/cooled water into high/low temperature reaction beds respectively for pre-cooling so that $M_H$ cooled down to $T_M$ and $M_L$ to $T_L$; then opened hydrogen valves again to start cooling period when $M_L$ absorbed $Q_L$ from cooled water and $M_H$ discharged $Q_{M2}$ to medium temperature oil. After the set time closed the oil and water valves, and began the next refrigeration cycle.

The high temperature oil bath was fixed as 453 K, the medium temperature oil and water were set around 293 K. The low temperature water bath was also set at about 293 K for simplification. The flow rates of heat conducting oil and water were 0.25 kg/m$^3$ respectively. Based on repeated tests, the operation time was set as 800 s for pre-heating, 850 s for regeneration, 650 s for pre-cooling and 1300 s for cooling period. Fig.6 shows the hydrides temperatures, the media temperatures at the inlet and outlet of the reaction beds as well as hydrogen pressure in one cycle. As shown in this figure, in the pre-heating process, HA and HB were heated to an average temperature of 423 K, while oil had a temperature drop of 8 K and hydrogen pressure rose from 100 kPa to 3 MPa. LA and LB pressures were maintained at around 100 kPa. When regeneration process began, the hydrogen pressure immediately reached balance at 920 kPa which was much lower than the equilibrium pressures of HA and HB at their bed temperatures, thus both quickly desorbed hydrogen and the average bed temperature sharply dropped down to 399 K; on the contrary, LA and LB quickly absorbed hydrogen with their average bed temperature rising to 319 K. In pre-cooling period, all beds were cooled, the hydrogen pressures decreased. HA and HB reached 60 kPa at the end of this period, while LA and LB were 620 kPa. When cooling period began, reaction beds met their balance again at 260 kPa, the average temperature of HA and HB increased quickly to 336 K, while that of LA and LB dropped to 273 K. The temperature difference between the inlet and outlet of the cooled water reached 2 K. With this process going on, the temperature of LA and LB gradually increased. The hydrogen pressure remained

at around 100 kPa, and the temperature difference of the cooled water gradually decreased.

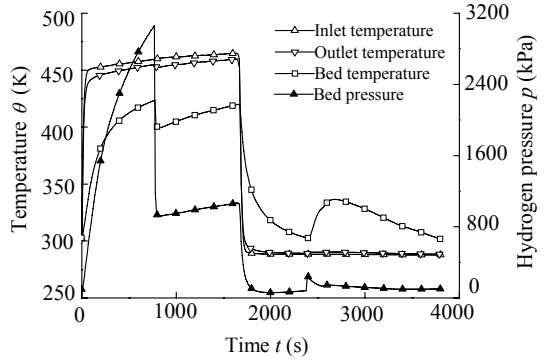


(a)

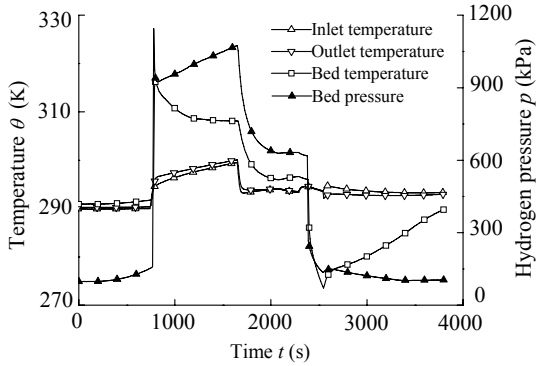


(b)

**Fig.6 Temperature and pressure of high (a) and low (b) temperature reaction beds**

Fig.7 showing the dynamic heating and cooling power reveals that both heating and cooling power decreases in each period, but heating power jumps sharply at the beginning of the regeneration period. The maximum heating power was 1320 W during the pre-heating period and 880 W during the regeneration period; the total heating quantity $Q_H$ of both periods was 1187 kJ, the average heating power of the two periods was 719 W and of the whole cycle was 330 W. The heating power per unit weight alloy was 30 W. The maximum cooling power of 639 W was achieved at the beginning of the refrigeration period; the total cooling quantity $Q_L$ was 309 kJ, the average cooling power of this period was 238 W; the average cooling power of the whole cycle was 84.6 W, the cooling power per alloy was merely 7.7 W/kg alloy. COP was calculated as 0.26. Since temperature changed slowly in most of the cycle except at the switching points of adjacent steps, the delay of measured temperature by thermal couples was neglected; therefore, the maximum relative error was 4.5% for heating quantity and 29.4% for cooling quantity.

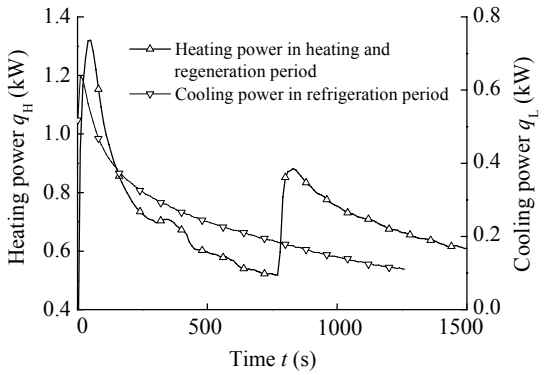


**Fig.7 Heating and cooling power in one cycle**

## Effect of driving heat source temperature

Fig.8 shows the effect of driving heat source temperature on system cooling power and COP with other cycle parameters invariable. With the decrease of heat source temperature, the total heating quantity, total refrigeration quantity, average cooling power and COP all decrease; The decrease of COP suggests that the drop of cooling quantity is much more serious than that of heating quantity. The cooling power was as low as 61 W at 424 K, which indicated that reaction speed is relatively slow at this temperature. Therefore, driving temperature should be high enough to ensure system basic function; on the other hand, the downwards bending curves in Fig.8 indicate that the enhancement of cooling power and COP becomes indistinct with the increase of driving temperature,

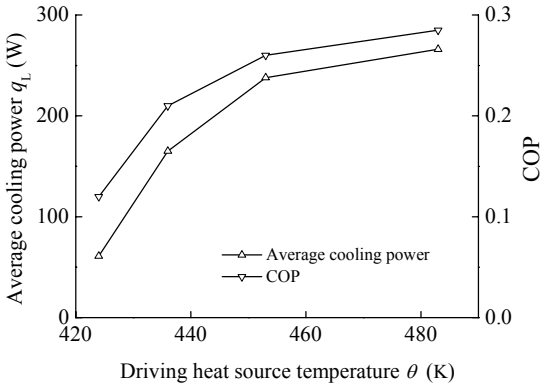


**Fig.8 Driving temperature effect**

thus excessive high driving temperature contributes less to cooling power evaluation. For this work pair, the optimum driving temperature is suggested to be 453 K.

**Effect of heat sink temperature**

Fig.9 shows the effect of heat sink temperature keeping other cycle parameters constant. For the same heat source temperature, heat rejection from reaction beds is depressed owing to the increase of heat sink temperature; hence both cooling power and COP decrease. When heat sink temperature rose to 323 K, the average cooling power was merely 32 W with COP being 0.1, indicating that system performance was seriously inferior.

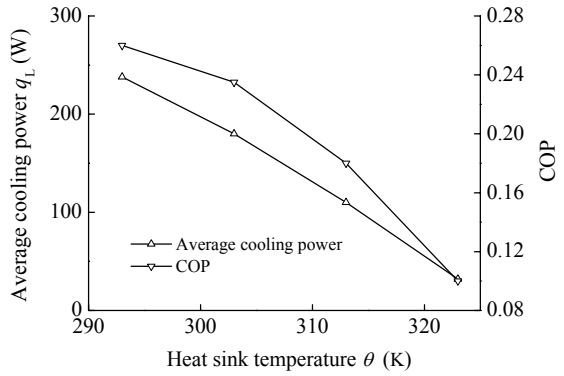


**Fig.9 Heat sink temperature effect**

**Effect of cycle time**

Cycle time is very important for a metal hydride cooling system. The influence of pre-heating and regeneration time as well as pre-cooling and refrigeration time is shown in Fig.10. In experiments on pre-heating and regeneration time, the ratio of pre-heating period to regeneration period remained around 1.0 while their summation varied from 1200 s to 2000 s; as for tests for pre-cooling and refrigeration time, the ratio of the former to the latter remained around 0.5 while their summation varied from 1500 s to 2400 s. It is seen that both cooling power and COP grows with the increase of pre-heating and regeneration time; COP increases while cooling power decreases with the elevation of pre-cooling and refrigeration time. The amount of hydrogen transferred increases with pre-heating and regeneration time, resulting in the increase of heat input and cold output; the increase of COP indicates that the latter has a more rapid increment than the former. The same thing happens for the cycle with elongated pre-cooling and refrigeration time, when average cooling power is reduced since hydrogen transfer rate gradually decreases during refrigeration.

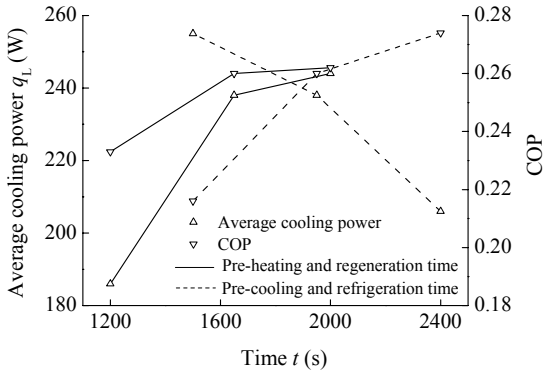


**Fig.10 Cycle time effect**

## DISCUSSION

This research developed a metal hydride work pair for exhaust gas driving automobile air conditioning systems. Testing of the hydriding properties confirmed that this hydride pair can meet practical requirement. Based on this work pair, a function proving automobile metal hydride intermittent refrigeration system was constructed, and intermittent refrigeration cycles were achieved. Experiments on the effect of driving heat source temperature, heat sink temperature and cycle time revealed that the reaction beds have satisfactory mass transfer performance; cooling power and system COP increase with the growth of heat source temperature as well as pre-heating and regeneration time while decreasing with heat sink temperature increment.

However, the bed equivalent thermal conductivities were not large enough, resulting in the excessive long cycling time and low cooling power. Further work will be focused on the optimization of bed structures to enhance heat transfer properties.

## References

Ahmed, S.S., Murthy, S.S., 2004. Analysis of a novel metal hydride cycle for simultaneous heating and cooling. *Renewable Energy*, **29**(4):615-631. [doi:10.1016/j.renene.2003.07.005]

Bedbak, S.S., Gopal, M.R., 2005. Performance analysis of a

compressor driven metal hydride cooling system. *Int. J. Hydrogen Energ.*, **30**(10):1127-1137. [doi:10.1016/j.ijhydene.2004.10.014]

Güther, V., Otto, A., 1999. Recent developments in hydrogen storage applications based on metal hydrides. *Journal of Alloys and Compounds*, **293-295**(1-2):889-892. [doi:10.1016/S0925- 8388(99)00385-0]

Izhvanov, L.A., Solovey, A.I., Frolov, V.P., 1996. Metal hydride heat pump-new type of heat converter. *Int. J. Hydrogen Energ.*, **21**(11-12):1033-1038. [doi:10.1016/S0360-3199(96)00046-8]

Kapischke, J., Hapke, J., 1998. Measurement of the pressure-composition isotherms of high-temperature and low-temperature metal hydrides. *Experimental Thermal and Fluid Science*, **18**(1):70-81. [doi:10.1016/S0894-1777(98)10007-9]

Kim, K.J., Montoya, B., Razani, A., 2001. Metal hydride compacts of improved thermal conductivity. *Int. J. Hydrogen Energ.*, **26**(6):609-613. [doi:10.1016/S0360-3199(00)00115-4]

Nakamura, H., Nakamura, Y., Fujitani, S., 1996. Cycle performance of a hydrogen-absorbing $La_{0.8}Y_{0.2}Ni_{4.8}Mn_{0.2}$ alloy. *Int. J. Hydrogen Energ.*, **21**(6):457-460. [doi:10.1016/0360-3199(95)00108-5]

Nakamura, H., Nakamura, Y., Fujitani, S., 1997. A method for designing a hydrogen absorbing $LaNi_{5-x-y}Mn_xAl_y$ alloy for a chemical refrigeration system. *Journal of Alloys and Compounds*, **252**(1-2):83-87. [doi:10.1016/S0925-8388(96)02611-4]

Oi, T., Maki, K., Sakaki, Y., 2004. Heat transfer characteristics of the metal hydride vessel based on the plate-fin type heat exchanger. *J. Power Sources*, **125**(1):52-61. [doi:10.1016/S0378-7753(03)00822-X]

Sánchez, A.R., Klein, H.P., Groll, M., 2003. Expanded graphite as heat transfer matrix in metal hydride beds. *Int. J. Hydrogen Energ.*, **28**(5):515-527. [doi:10.1016/S0360-3199(02)00057-5]

Srivastava, S., Srivastava, O.N., 1999. Synthesis, characterization and hydrogenation behaviour of composite hydrogen storage alloys: $LaNi_5/La_2Ni_7$, $LaNi_3$. *Journal of Alloys and Compounds*, **282**(1-2):197-203. [doi:10.1016/S0925-8388(98)00741-5]

Willers, E., Groll, M., 1999. Evaluation of metal hydride machines for heat pumping and cooling applications. *Int. J. Refrig.*, **22**(1):47-58. [doi:10.1016/S0140-7007(97)00056-X]